## Title
A pose-independent method for accurate and precise body composition from 3D optical scans



## Journal
Obesity, 29(11)

## ISSN
1930-7381

## Authors
Wong, Michael C
Ng, Bennett K
Tian, Isaac
et al.

## Publication Date
2021-11-01

## DOI
10.1002/oby.23256

Peer reviewed

HHS Public Access

Author manuscript

*Obesity (Silver Spring)*. Author manuscript; available in PMC 2022 November 01.

Published in final edited form as:

*Obesity (Silver Spring)*. 2021 November ; 29(11): 1835–1847. doi:10.1002/oby.23256.

# A Pose Independent Method for Accurate and Precise Body Composition from 3D Optical Scans

**Michael C Wong**[1,2], **Bennett K Ng**[3], **Isaac Tian**[5], **Sima Sobhiyeh**[4], **Ian Pagano**[2], **Marcelline Dechenaud**[4], **Samantha F Kennedy**[4], **Yong E Liu**[2], **Nisa Kelly**[2], **Dominic Chow**[6], **Andrea K Garber**[7], **Gertraud Maskarinec**[2], **Sergi Pujades**[8], **Michael J Black**[9], **Brian Curless**[5], **Steven B Heymsfield**[4], **John A Shepherd**[1,2]

[1]Graduate Program in Human Nutrition, University of Hawai'i Manoa, Honolulu, Hawaii, USA

[2]University of Hawai'i Cancer Center, Honolulu, Hawaii, USA

[3]Intel Corp. Santa Clara, California, USA

[4]Pennington Biomedical Research Center, Louisiana State University, Baton Rouge, Louisiana, USA

[5]Paul G. Allen School of Computer Science and Engineering, University of Washington, Seattle, Washington, USA

[6]John A. Burns School of Medicine, University of Hawai'i, Honolulu, Hawaii, USA

[7]University of California, San Francisco, California, USA

[8]Inria, Univ. Grenoble Alpes, CNRS, Grenoble INP, LJK, Grenoble, FRANCE

[9]Max Planck Institute for Intelligent Systems, Tübingen, Germany

## Abstract

**Objective:** To investigate if digitally reposing three-dimensional optical (3DO) whole-body scans to a standardized pose would improve body composition accuracy and precision regardless of initial pose.

**Methods:** Healthy adults (n=540), stratified by sex, BMI, and age, completed whole-body 3DO and dual-energy X-ray absorptiometry (DXA) scans in the Shape Up! Adults study. The 3DO mesh vertices were represented with standardized templates and a low-dimensional space by principal component analysis (stratified by sex). Total sample was split into a training (80%) and test (20%) set for both males and females. Stepwise linear regression was used to build prediction models for body composition and anthropometry outputs using 3DO principal components (PCs).

**Address correspondence to:** John A. Shepherd, Ph.D., University of Hawai'i Cancer Center, 701 Ilalo Street, Honolulu, Hawai'i 96813. johnshep@hawaii.edu.

AUTHOR CONTRIBUTIONS

JAS and MCW designed and conducted the research; YEL, NNK, SFK, and MCW collected data from participants; JAS, IP, SS, and MCW analyzed the data; all authors contributed to the text of the manuscript; MCW and JAS drafted the manuscript and had primary responsibility over the final content. All authors reviewed and approved the final manuscript.

**Clinical Trial Registration:** ClinicalTrials.gov Identifier no. NCT03637855

**Disclosure:** All authors have no conflicts of interest to disclose.

**Results:** The analysis included 472 participants after exclusions. After reposing, three PCs described 95% of the shape variance in the male and female training sets. 3DO body composition accuracy compared to DXA was: fat mass $R^2$ = 0.91 male, 0.94 female; fat-free mass $R^2$ = 0.95 male, 0.92 female; visceral fat mass $R^2$ = 0.77 male, 0.79 female.

**Conclusions:** Reposed 3DO body shape PCs produced more accurate and precise body composition models that may be used in clinical or nonclinical settings when DXA is unavailable or when frequent ionizing radiation exposure is unwanted.

### Keywords

Imaging; Principal Component Analysis; Body Composition; Dual Energy X-ray Absorptiometry; Obesity; Metabolic Disease; 3D scanning; Body Shape

## INTRODUCTION

Obesity has been a growing problem in the United States (1) and worldwide (2). Obesity is accompanied by metabolic diseases (3), cardiovascular disease (4), and up to 20% of cancers (5). Obesity is generally classified using body mass index (BMI), but BMI does not account for muscle mass, and therefore, it is a poor method for nutritional assessment on an individual level. Instead, anthropometric and regional body composition measurements have been shown to be better predictors of metabolic diseases and mortality risk than BMI (6, 7). However, these methods have their own limitations.

Anthropometric tape measurements require experienced technicians, can be time consuming, and may feel invasive for patients with obesity or eating disorders (8, 9). There may also be human bias with repeat anthropometric tape measurements as humans may tend to aim for their previous measurement. Criterion body composition methods for whole-body and/or regional body composition, such as dual-energy X-ray absorptiometry (DXA), MRI and CT require highly trained personnel, uses ionizing radiation (DXA and CT), have high cost, and may not be as accessible in certain areas (10). Bioelectrical impedance analysis (BIA) is also commonly used and is broadly available, but the agreement with criterion methods varies between systems (11, 12). An ideal method would include both regional body composition, automated anthropometry, be low cost, have little to no training requirements to operate, and be accurate to criterion measures relevant to metabolic risk.

In recent years, three-dimensional optical (3DO) scanners have been shown to meet the above ideal criteria (13, 14). 3DO scanners are readily available in fitness centers throughout the world. Whole body scanning can also be performed with consumer 3DO cameras primarily sold for gaming. Several smart phones also have depth cameras capable of creating accurate 3DO images (15). 3DO scanners have shown to output accurate and precise estimates of circumferences, surface areas, and volumes (16, 17, 18). 3DO scanners do not emit ionizing radiation, scan time is short, cost less than DXA, can be used as frequently as needed, and self-administered. They also generate faster results and can measure interesting health indices (e.g., whole-body and regional surface areas and volumes) that would be time consuming to produce manually.

3DO scanners output a high-resolution 3D mesh that portrays detailed body shape. In a previous study, investigators used the high-resolution 3D meshes and built statistical shape models to predict body composition in respects to dual-energy X-ray absorptiometry (DXA) (19). The statistical shape models were created to describe complex shape features including height, regions of adiposity accumulation, and muscle tone. Investigators reported that their shape models predicted body composition with better accuracy than BMI or anthropometrics (19). However, in the previous study, these 3DO scans contained variation in positioning and pose. Although people naturally have different positioning and pose due to posture and balance, this introduces unwanted variance in the shape models. Since the scanner used in Ng et al. (19) had fixed telescoping handle bars, participants had their arms abducted from the torso, in an A-pose. The distance and angle of the arm relative to the torso will vary. Furthermore, participants that struggle with balance may be leaning back, forward, or shifting their weight to their dominant side when the 3DO platform rotates. The unwanted pose variance can bias the model's accuracy and precision. If pose variance is removed from the raw scan by standardizing everyone's pose, the shape models may be more representative of shape, exclude noise that has nothing to do with shape, and can estimate body composition more accurately and precisely.

The primary objective of this study was to investigate if removing pose variations generate statistical shape models with higher accuracy and precision for body composition models than models with pose included (19). The secondary objective was to explore the robustness of the pose-invariant models using scans that would normally be rejected due to their poor pose conformity.

## METHODS

### Study Design

Shape Up! Adults is an ongoing cross-sectional study of healthy adults (NIH R01 DK109008, ClinicalTrials.gov ID NCT03637855). This study was designed to investigate the associations between body shape and composition with various health indices. Participants underwent whole-body 3DO scans, whole-body dual energy X-ray absorptiometry (DXA) scans, blood serum tests, and function tests for hand grip and knee extension strength.

### Participants

Participants (n=540) were recruited at Pennington Biomedical Research Center (PBRC), University of Hawaii Cancer Center (UHCC), and University of California, San Francisco (UCSF). All participants provided informed consent. The study protocol was approved by the Institutional Review Boards (IRBs) at PBRC (IRB study #2016-053), UCSF (IRB #15-18066), and the University of Hawaii Office of Research Compliance (UH ORC, CHS #2017-01018). Volunteers were pre-screened over the phone and were deemed ineligible if they were pregnant, breastfeeding, had missing limbs, non-removable metal, previous body-altering surgery, hair that could not be contained in a swim cap, or were unable to stand still for one minute. Pretesting preparations included an eight-hour fast (water and prescribed medications were allowed) and no strenuous exercise 24 hours prior to the study visit.

Participants were stratified by age (18-40, 40-60, >60 years), ethnicity (non-Hispanic white, non-Hispanic black, Hispanic, Asian, and Native Hawaiian or Pacific Islander (NHOPI)), sex, and BMI (<18, 18-25, 25-30, >30 kg/m$^2$). Height and weight were taken on a SECA 274 Stadiometer (SECA GmbH, Hamburg, Germany). Manual anthropometric measures (arm, thigh, waist, and hip circumferences) were taken with anthropometry tape following National Health and Nutrition Examination Survey (NHANES) standard protocol (20).

### 3D Optical Surface Scan Acquisition

Participants changed into form-fitting tights, a sports bra if female, and a swim cap. Duplicate 3DO surface scans were taken with the Fit3D Proscanner version 4.x (Fit3D Inc., San Mateo, CA, USA) using a standardized A-pose positioning protocol, where participants grasped the telescoping handles on the scanner platform, stood up straight with shoulders relaxed and arms positioned straight and abducted from their body (Figure S1A). Duplicate scans were taken within 15 minutes of the first (with repositioning). The platform rotates once around and takes approximately 45 seconds. The Iterative Closest Point (ICP) algorithm was applied to spatially align point clouds captured by the cameras as the subject rotates (21). Final point clouds were converted to a mesh connected by triangles with approximately 300,000 vertices and 600,000 faces to represent body shape. All 3DO scans taken on the Fit3D Proscanner were transferred to Fit3D, who securely transferred the data to UHCC for statistical analysis. Along with the mesh, Fit3D provided digital anthropometry (circumferences, lengths, volumes, and surface areas).

To test the robustness of our models (Figure 1), four female and four male participants were scanned four times in succession in various alterations of the standard A-pose to mimic real world positioning problems (e.g., leaning forward, squatting, leaning to side, bent knee). The goal of these scans is to test how stable the body composition and anthropometry estimates are in the presence of positioning problems. This will be referred to as the stability test for the remainder of this paper.

### 3D Optical Surface Scan Analysis

There were two different analyses done with the 3DO scans, A-pose and T-pose. These refer to two different methods and were not direct measurements. For the A-pose analysis, a standardized 60,000-vertex mesh template was warped to fit each participant's 3DO scan using methods of Allen et al. (22). This registration allows for direct anatomical 3DO body shape comparison of the whole sample. Seventy-five fiducial points were placed manually on anatomical landmarks described by the Civilian American and European Surface Anthropometry Resource Project (CAESAR) (23). Marker placement was performed by trained and validated in-house personnel using Meshlab 1.3.2 (Consiglio Nazionale delle Ricerche, Rome, Italy). Using the software developed by Allen et al., the template's markers were transformed to the target mesh's markers. Then the vertices from the template were warped to fit the target mesh's shape (19, 22). The result of this procedure produced meshes with exactly 60,000 vertices that correspond across all the meshes.

For the T-pose analysis, data obtained from the raw A-pose mesh was used in this analysis. There was no additional scan taken. The raw mesh files were sent to Meshcapade

(Meshcapade GmbH, Tubingen, Germany) to be digitally reposed. The Meshcapade algorithm takes as input a raw 3D body scan containing an arbitrary number of unordered vertices and produces as output a registered water-tight 110,000-vertex mesh with full anatomical correspondence. This means that each numbered vertex corresponds to a specific anatomical location across all registered meshes and are no longer random. The meshes were reposed and represented each individual in a standardized T-pose. For the current analysis, reposing means the arms were brought horizontal and in plane with the body, legs and arms straightened, and torso upright (Figure 1). The hands, feet, and face of the individual are replaced with stylized equivalents, artistic renderings of sites that generally have lower resolution compared to the rest of the body. Meshcapade's methods are described in detail by Loper et al. (24). Unlike Fit3D, Meshcapade does not have volumes or surface area estimates. In order to have these estimates available, prediction models were created.

## Dual-energy X-ray Absorptiometry

Participants received two whole-body DXA scans with repositioning on either a Hologic Horizon/A system at UCSF or a Discovery/A system at PBRC or UHCC (Hologic Inc., Marlborough, MA, USA). Scans were taken according to International Society for Clinical Densitometry guidelines (25). DXA cross-calibration phantoms were circulated between all sites and calibration equations were derived to remove systematic bias in all bone and soft tissue results. All DXA scans were centrally analyzed by a single certified technologist using Hologic Apex version 5.6 with the NHANES Body Composition Analysis calibration option disabled. The output from the DXA scan included regional and whole-body composition.

## Statistical Analysis

The total study sample was randomly divided into a training set (80%) and test set (20%). A two-sided student's *t*-test was used to describe differences between sets' demographics. Pearson correlation coefficients were calculated between body composition and anthropometry (Table S1 and Table S2). *P*-values $< 0.05$ were considered statistically significant.

As the coordinates of each point in a regular 3D body mesh are highly correlated to the neighboring vertices, principal component analysis (PCA) was applied to reduce the dimensionality and orthogonalize the 3D mesh data (22). The resulting principal components (PCs) were used as predictors for body composition.

Synthesized body shapes were generated to visualize the variance represented by each PC (Figure 2). Mean male and female body shapes were calculated by averaging the mesh point coordinates across all individual meshes in the sample. Mean centering was performed as part of the PCA, such that the origin of the PC space (where all PC weights equal zero) corresponds to the mean body shape. High (+3 standard deviations [SD]) and low (−3 SD) states of each PC were generated by varying each PC separately with all others held as equal to zero. These PC weight vectors were inverted back to Cartesian space and added to the sex-specific mean body shape for visualization (26).

Stepwise forward linear regressions with five-fold cross validation were used to generate sex-specific prediction models for outcomes of body composition, volumes, and total surface

area, in the training set. The dependent variables were the body composition, volumes, and total surface area. The independent variables were the PCs and anthropometry. Four model types were created in this study: (1) “T-pose PC-only” models that included the first fifteen T-pose PCs as variable candidates and (2) “T-pose PC + Anthro” models that included the first fifteen PCs and manual anthropometry (waist, hip, arm, and thigh circumferences; height; weight; BMI; waist-to-hip ratio; waist-to-height ratio) as variable candidates. An additional two model types using methods from Ng et al. 2019 (19), (3) “A-pose PC-only” and (4) “A-pose PC + Anthro”, were recreated within the same samples as in this manuscript to specifically understand the effects of pose on the modeling results. Accuracy of each model was quantified with the coefficient of determination ($R^2$) and root mean square error (RMSE). Total surface area was calibrated to Tikuisis’ body surface area equations (27). Volumes were calibrated to DXA derived volumes (28). Equations were built on the training set and validated on the test set. Models were chosen using the SAS GLMSELECT procedure in SAS v.9.4 (SAS Institute, Cary, NC).

Predicted total fat mass was calculated using the derived stepwise linear regression equation, predicted total fat-free mass by subtracting the predicted fat mass from measured scale weight, and predicted percent fat by dividing the predicted fat mass by measured scale weight. Table S3 and Table S4 provides predictor and coefficients for females and males, respectively.

The scans taken on four female and four male participants in variations of A-poses were reposed to the T-pose for the stability test (Figure 3). Body composition and anthropometry were estimated for the A-pose and T-pose meshes by their respective PC model. The properly positioned A-pose and its T-pose derivation were used as the criterion meshes for comparison to the three alternative poses. Differences of body composition, total volume, and total surface area between the standard A-pose mesh and the alternative poses were plotted in a box and whisker plot to show the robustness of our method. Bland-Altman plots (Figure 4) were used to show potential biases in our T-pose body composition models (29).

Duplicate 3DO and DXA scans were used for the test-retest precision analysis. Coefficient of variation (CV) and RMSE were used to quantify the test-retest precision as defined by Gluer (30). The precision error of the 3DO estimates was calculated for both A-pose and T-pose.

Test set 3DO meshes were transformed into PC space by using the established PCA model from the training set. Models built from stepwise linear regression (mentioned above) were validated on this external set of meshes in order to evaluate generalizability of the body composition, volumes, and total surface area models.

PCA, PC images, and the model stability test were generated using R version 4.0.2 (R Core Team). All other statistical analysis was performed on SAS version 9.4 (SAS Institute, Cary, NC, USA). Sample code and instructions to rederive body composition metrics using the T-pose mesh can be found here: https://github.com/MikeWong510/T-pose-PCA-Body-Composition.

# RESULTS

## Participants

Five hundred forty participants had completed the study at the time of the analysis. Nineteen participants were excluded for invalid DXA scans (9 had body parts off the field of view, 9 had high density artifacts, and 1 had a movement artifact). Three participants dropped out of the study. Forty-seven participants were excluded for invalid 3DO scans (20 did not have appropriate attire, 15 scans had manufacturing errors, and 12 had movement artifacts). After these exclusions, 474 participants (UCSF = 155, PBRC = 269, and UHCC = 50) remained in the analysis. There were no significant demographic differences between the training and test sets (all $p > 0.10$) for males and females. Descriptive characteristics of the study sample (training set) are shown in Table 1 and by ethnicity in Table S5.

## Shape Models

PCA on reposed 3DO meshes created statistical shape models for both sexes. Three PCs captured 95% of the shape variance in each of the male and female shape models. Male and female mean body shapes and visualization of the PCs (±3 SD for each PC from the average shape) for males and females are presented in Figure 2. Univariate correlations of each PC to health metrics are presented in Table S1 and Table S2.

For both the male and female shape models, PC2 was significantly correlated to all body composition measures PC3 had similar relationships to body composition markers, although not as strong as PC2.

## Prediction Equations

Body composition models using the T-pose PC-only improved modestly compared to A-pose PC-only model in terms of $R^2$ and RMSE (Table 2). T-pose PC-only models for male body composition had $R^2$ values that ranged from 0.70 to 0.95, while females ranged from 0.71 to 0.95. T-pose percent fat improved for males ($R^2$ from 0.64 to 0.70; RMSE from 3.70% to 3.36%) and females ($R^2$ from 0.66 to 0.71; RMSE 4.32% to 3.96%) compared to A-pose. The most substantial improvement was the visceral fat estimate in T-pose for males ($R^2$ from 0.64 to 0.78; RMSE 0.17 kg to 0.13 kg), while females had only a modest improvement ($R^2$ from 0.73 to 0.78; RMSE 0.14 kg to 0.13 kg). All models improved when BMI and other anthropometric measures were used as possible covariates in the stepwise regression models. BMI was a significant predictor of total fat in females but not in males.

T-pose PC-only equations predicted total surface area and regional and total volume with high accuracy. Although results were comparable for both poses, T-pose had slightly higher $R^2$ values and lower RMSE in the regional volume estimates.

## Stability Test

A-pose body composition and anthropometry had wider ranges and outliers on the box and whisker plots compared to the T-pose (Figure 3). The eight subjects were between 26-80 years of age. Five had normal, two had overweight, and one had obese BMI classifications.

### Bland-Altman Analysis

Overall, there was a fairly even distribution across the Bland-Altman plots (Figure 4). Most of the points are within the confidence intervals with a few outliers. Best-fit lines were included in each plot to examine potential biases. Fat mass had a slight bias in the heavier and lighter subjects for both males and females, possibly due to the smaller sample in both extremes. However, the fat-free mass and percent fat plots showed little bias in either direction.

After seeing a slight bias on the side with obesity, additional analysis (Table S6) was done to determine the accuracy in the subgroup with obesity. Total fat mass in the females with obesity (n=59) and males with obesity (n=47) training samples (BMI > 30) achieved similar results ($R^2$, 0.91 and 0.91; RMSE, 3.53 kg and 3.07 kg, respectively) to the whole training sample.

### Test-Retest Precision

For total fat mass, DXA (CV, 1.33 and 0.95; RMSE, 0.25 kg and 0.23 kg) had better precision than T-pose (CV, 2.37 and 2.24; RMSE, 0.44 kg and 0.55 kg) for males and females, respectively (Table 3). Visceral fat by T-pose (CV, 4.99 and 4.64; RMSE, 0.02 kg and 0.02 kg) had better precision than DXA (CV, 7.36 and 7.91; RMSE, 0.03 kg and 0.03 kg) in males and females, respectively. Across the board, T-pose had better test-retest precision than A-pose for body composition and anthropometry.

### Test Set

The T-pose test set results were similar to the training set for males and females (Table 4). The male A-pose test set results did not perform as well as the training in regards to total body estimates. However, regional composition results, PC+Anthro models, total surface area, and regional and total volume results were comparable.

## DISCUSSION

For this study, PCA on reposed 3D body meshes described body shape variance across a diverse sample and were compared to the A-pose PC models described previously (19). In this study, three PCs described 95% of the variance of body shape in the training sample, compared to eleven PCs in Ng et al. Reposing the meshes to a standardized pose took away most, if not all, of the variance pertaining to pose, leaving mainly shape variance. The removal of pose variance helped create more accurate and precise models, which may allow for better body composition monitoring for clinical purposes. From these findings, we recommend using the T-pose models over the previously published Ng et al. models (19).

When examining the first three PCs at +/− 3 standard deviations (Figure 2), the shape variance explained was similar in males and females. Consistently for male and female models, the first PC seemed to describe height and body size, second PC described adiposity, third PC also described adiposity but with a weaker signal, and fourth and fifth PC both describe abdominal adiposity and muscle tone. When comparing to Ng et al. (19), the first PC looked to described height and body size, the second PC had a noticeable forwards

and backwards lean, and the third PC had strong signals for adiposity in both males and females. By reposing the meshes to a standardized pose (T-pose), variance in pose, such as the forwards and backwards lean, was eliminated from the PCs.

In comparison to other body composition modalities, our body composition method validated well to DXA assessments. Beeson et al. reported $R^2$ for males and females combined for fat mass, fat-free mass, and percent fat ($R^2$s; 0.91, 0.90, and 0.83, respectively) when using a Tanita Bioelectrical Impedance Analysis (BIA) unit (31). Frisard et al. examined the agreement between air displacement plethysmography (ADP) compared to DXA and reported fat mass, fat-free mass, and percent fat ($R^2$s; 0.83, 0.91, and 0.83, respectively) (32). Compared to these studies, T-pose 3D body shape PC models exhibited slightly better fat mass and fat-free mass agreement with DXA.

When examining the subgroup with obesity (BMI > 30), female total fat mass had a slightly lower $R^2$ and 0.65 kg increase in RMSE compared to the whole training sample. The Male obesity group's total fat mass had almost identical statistics. In the Bland-Altman plots (Figure 4), most individuals are within the confidence intervals. There were two points beyond the confidence intervals when examining males and females with a mean total fat mass > 40 kg. The slight bias in the extremely obese group may be attributed to the low sample size of the subgroup.

T-pose PC-only test-retest precision results were better than A-pose PC-only across the board. Only female arm fat and arm lean were outperformed by A-pose. Since the methods were the same for females and males, the reasoning is not completely clear. Some of the T-pose test-retest results were better than DXA (e.g., male and female visceral fat, trunk lean, and male arm fat). One technique to reduce the precision error to that of DXA and to track smaller changes of body composition over time would be to average multiple scans taken in succession. The precision in the estimate improves by the square root of the number of scans (e.g., the average of four scans would lower the male fat mass precision error from 0.44 kg to 0.22 kg).

T-pose validations were consistently better than A-pose in males (most notably, male whole-body and visceral fat). For females, the A-pose and T-pose validated similarly across all outcomes. A notable female outcome that was better in T-pose ($R^2 = 0.76$) than A-pose ($R^2 = 0.72$) was visceral fat. From the wide range of the sample, the models created are robust and may validate well with other populations.

One of the highlights was the model's robustness to significant pose variability. Although only four females and four male participants were used in this exercise (Figure 3), it can be seen that the T-pose body composition and anthropometry models produced more precise estimates compared to the conventional A-pose method when pose differences are extreme. Though there was improvement using the T-pose method, this exercise was only done on eight people and the amount of improvement may vary for different individuals. When using the A-pose PC-only equations, the participants had body composition estimates that were over double the criterion scan, which shows the A-pose method is unreliable when the participants were outside the manufacturer's recommended pose protocol.

This study had several strengths. First, the study sample was highly stratified by age, sex, ethnicity, and BMI. This provided an abundance of shape variance to create more encompassing models that could be used across many healthy populations. In comparison to using a few sub regions with anthropometric tape measures, PCA allows the user to incorporate the entire body for statistical shape models. By taking pose out of the PCA model, the variance left to describe was shape, which allowed for a more accurate representation of a shape-oriented model. Furthermore, an addition of a test set allowed us to check for generalizability. Lastly, by using the Meshcapade's software described by Loper et al. (24), laborious, manual landmark placement was completely avoided (19).

The study is not without limitations. The study sample was restricted to healthy individuals without any known diseases. Individuals with body shape altering symptoms (e.g., muscle wasting or severe edema), are not advised to use these models. Lastly, the models in this study were built using a specific 3D body scanner (the Fit3D ProScanner).

## Conclusion

In conclusion, PCA of reposed 3DO meshes eliminated most, if not all, of the pose variance in the PCA model. The reposing helped create more stable models that can predict a person's body composition regardless of initial pose. To date, this is the first analysis that used scans without pose variation for body composition and showed our models are robust even if scans were taken in poses outside manufacturer protocol. As 3DO scanners are becoming more readily available and affordable, this study further shows the potential and need for further development of 3DO for health and nutrition assessment. A person can scan themselves, the scan is reposed and standardized to the shape model, and the user receives their body composition and other health metrics within a matter of minutes.

## Supplementary Material

Refer to Web version on PubMed Central for supplementary material.

## ACKNOWLEDGMENTS

We give a big thank you to all the participants for graciously giving us their time for this study, Tyler Carter and Greg Moore at Fit3D for providing us the 3DO data, Naureen Mahmood and Talha Zaman at Meshcapade for providing us the application program interface to repose our 3DO data, and Geraldine Ragsac for helping us piece together images for our figures. We would also like to thank our collaborators from San Francisco, Honolulu, Baton Rouge, and Seattle for their part in the study. The data underlying this study cannot be made publicly available because the data contains patient identifying information. Data is available from the Shape Up! Studies for researchers who meet the criteria for access to confidential data. For details and to request an application, please contact John Shepherd johnshep@hawaii.edu or visit www.shapeup.shepherdresearchlab.org.

**Funding:**

Phases of this study were funded by the National Institute of Diabetes and Digestive and Kidney Diseases (NIH R01 DK R01DK109008) and The Translational Research Institute for Space Health (NNX16AO69A-FIP0017)

## REFERENCES


1. Hales CM, Fryar CD, Carroll MD, Freedman DS, Ogden CL. Trends in obesity and severe obesity prevalence in US youth and adults by sex and age, 2007-2008 to 2015-2016. JAMA 2018;319: 1723–1725. [PubMed: 29570750]
2. James PT. Obesity: the worldwide epidemic. Clinics in Dermatology 2004;22: 276–280. [PubMed: 15475226]
3. Després J-P, Lemieux I. Abdominal obesity and metabolic syndrome. Nature 2006;444: 881. [PubMed: 17167477]
4. Grundy SM. Obesity, metabolic syndrome, and cardiovascular disease. The Journal of Clinical Endocrinology & Metabolism 2004;89: 2595–2600. [PubMed: 15181029]
5. Calle EE, Rodriguez C, Walker-Thurmond K, Thun MJ. Overweight, obesity, and mortality from cancer in a prospectively studied cohort of US adults. New England Journal of Medicine 2003;348: 1625–1638.
6. Jacobs EJ, Newton CC, Wang Y, Patel AV, McCullough ML, Campbell PT, et al. Waist circumference and all-cause mortality in a large US cohort. Archives of Internal Medicine 2010;170: 1293–1301. [PubMed: 20696950]
7. Kuk JL, Katzmarzyk PT, Nichaman MZ, Church TS, Blair SN, Ross R. Visceral fat is an independent predictor of all-cause mortality in men. Obesity 2006;14: 336–341. [PubMed: 16571861]
8. Andrews ET, Ashton JJ, Pearson F, Beattie RM, Johnson MJ. Handheld 3D scanning as a minimally invasive measuring technique for neonatal anthropometry. Clinical Nutrition ESPEN 2019;33: 279–282. [PubMed: 31451267]
9. Haleem A, Javaid M. 3D scanning applications in medical field: a literature-based review. Clinical Epidemiology and Global Health 2019;7: 199–210.
10. Cherry SR, Sorenson JA, Phelps ME. Physics in Nuclear Medicine e-Book. Elsevier Health Sciences, 2012.
11. Achamrah N, Colange G, Delay J, Rimbert A, Folope V, Petit A, et al. Comparison of body composition assessment by DXA and BIA according to the body mass index: A retrospective study on 3655 measures. PloS One 2018;13: e0200465. [PubMed: 30001381]
12. Burns RD, Fu Y, Constantino N. Measurement agreement in percent body fat estimates among laboratory and field assessments in college students: Use of equivalence testing. PloS One 2019;14: e0214029. [PubMed: 30893355]
13. Heymsfield SB, Bourgeois B, Ng BK, Sommer MJ, Li X, Shepherd JA. Digital anthropometry: a critical review. European Journal of Clinical Nutrition 2018;72: 680. [PubMed: 29748657]
14. Heymsfield SB, Stevens J. Anthropometry: continued refinements and new developments of an ancient method. The American Journal of Clinical Nutrition. 2017 1;105(1):1–2. [PubMed: 28003202]
15. Kennedy S, Hwaung P, Kelly N, Liu YE, Sobhiyeh S, Heo M, et al. Optical imaging technology for body size and shape analysis: evaluation of a system designed for personal use. European Journal of Clinical Nutrition 2020;74: 920–929. [PubMed: 31551533]
16. Bourgeois B, Ng B, Latimer D, Stannard C, Romeo L, Li X, et al. Clinically applicable optical imaging technology for body size and shape analysis: comparison of systems differing in design. European Journal of Clinical Nutrition 2017;71: 1329. [PubMed: 28876331]
17. Ng B, Hinton B, Fan B, Kanaya A, Shepherd J. Clinical anthropometrics and body composition from 3D whole-body surface scans. European Journal of Clinical Nutrition 2016;70: 1265. [PubMed: 27329614]
18. Wong MC, Ng BK, Kennedy SF, Hwaung P, Liu EY, Kelly NN, et al. Children and Adolescents' Anthropometrics Body Composition from 3-D Optical Surface Scans. Obesity 2019;27: 1738–1749. [PubMed: 31689009]
19. Ng BK, Sommer MJ, Wong MC, Pagano I, Nie Y, Fan B, et al. Detailed 3-dimensional body shape features predict body composition, blood metabolites, and functional strength: the Shape Up! studies. The American Journal of Clinical Nutrition 2019.

20. Control CfD, Prevention. National Health and Nutrition Examination Survey (NHANES) Anthropometry Procedures Manual. US Department of Health and Human Services, Centers for Disease Control and Prevention 2013.
21. Besl PJ, McKay ND. Method for registration of 3-D shapes. Sensor fusion IV: control paradigms and data structures. International Society for Optics and Photonics, 1992, pp 586–606.
22. Allen B, Curless B, Popović Z. The space of human body shapes: reconstruction and parameterization from range scans. ACM Transactions on Graphics (TOG) 2003;22: 587–594.
23. Robinette KM, Blackwell S, Daanen H, Boehmer M, Fleming S. Civilian american and european surface anthropometry resource (caesar), final report. volume 1. summary. SYTRONICS INC DAYTON OH, 2002.
24. Loper M, Mahmood N, Romero J, Pons-Moll G, Black MJ. SMPL: A skinned multi-person linear model. ACM Transactions on Graphics (TOG) 2015;34: 248.
25. Hangartner TN, Warner S, Braillon P, Jankowski L, Shepherd J. The Official Positions of the International Society for Clinical Densitometry: acquisition of dual-energy X-ray absorptiometry body composition and considerations regarding analysis and repeatability of measures. Journal of Clinical Densitometry 2013;16: 520–536. [PubMed: 24183641]
26. Tian IY, Ng BK, Wong MC, Kennedy S, Hwaung P, Kelly N, et al. Predicting 3D Body Shape and Body Composition from Conventional 2D Photography. Medical Physics 2020.
27. Tikuisis P, Meunier P, Jubenville C. Human body surface area: measurement and prediction using three dimensional body scans. European Journal of Applied Physiology 2001;85: 264–271. [PubMed: 11560080]
28. Wilson JP, Mulligan K, Fan B, Sherman JL, Murphy EJ, Tai VW, et al. Dual-energy X-ray absorptiometry–based body volume measurement for 4-compartment body composition. The American Journal of Clinical Nutrition 2012;95: 25–31. [PubMed: 22134952]
29. Bland JM, Altman D. Statistical methods for assessing agreement between two methods of clinical measurement. The Lancet 1986;327: 307–310.
30. Gluer CC, Blake G, Lu Y, Blunt BA, Jergas M, Genant HK. Accurate assessment of precision errors: how to measure the reproducibility of bone densitometry techniques. Osteoporosis International 1995;5: 262–270. [PubMed: 7492865]
31. Beeson W, Batech M, Schultz E, Salto L, Firek A, Deleon M, et al. Comparison of body composition by bioelectrical impedance analysis and dual-energy X-ray absorptiometry in Hispanic diabetics. International Journal of Body Composition Research 2010;8: 45. [PubMed: 21318088]
32. Frisard MI, Greenway FL, DeLany JP. Comparison of methods to assess body composition changes during a period of weight loss. Obesity Research 2005;13: 845–854. [PubMed: 15919837]

**What is already known about this subject?**

1. Body shape by 3D optical can accurately and precisely estimate body composition.
2. There are strong correlations between body shape and body composition, anthropometric measures, blood biomarkers, and strength.

**What are the new findings in your manuscript?**

1. Body shape models are influenced by the participant's pose in the 3D optical scan and introduce noise that decreases the accuracy and precision of body composition estimates.
2. If 3D optical scans are reposed to a standardized pose, the body composition estimates will be more accurate and precise.

**How might your results change the direction of research or the focus of clinical practice?**

1. 3D optical imaging is becoming more accessible and has been proposed as an alternative to manual anthropometry and body composition measures. Our results show a standardizing method to improve upon established methods in order to obtain the most accurate and precise estimates. This is critical to clinical practices that use metrics such as body composition and anthropometry.

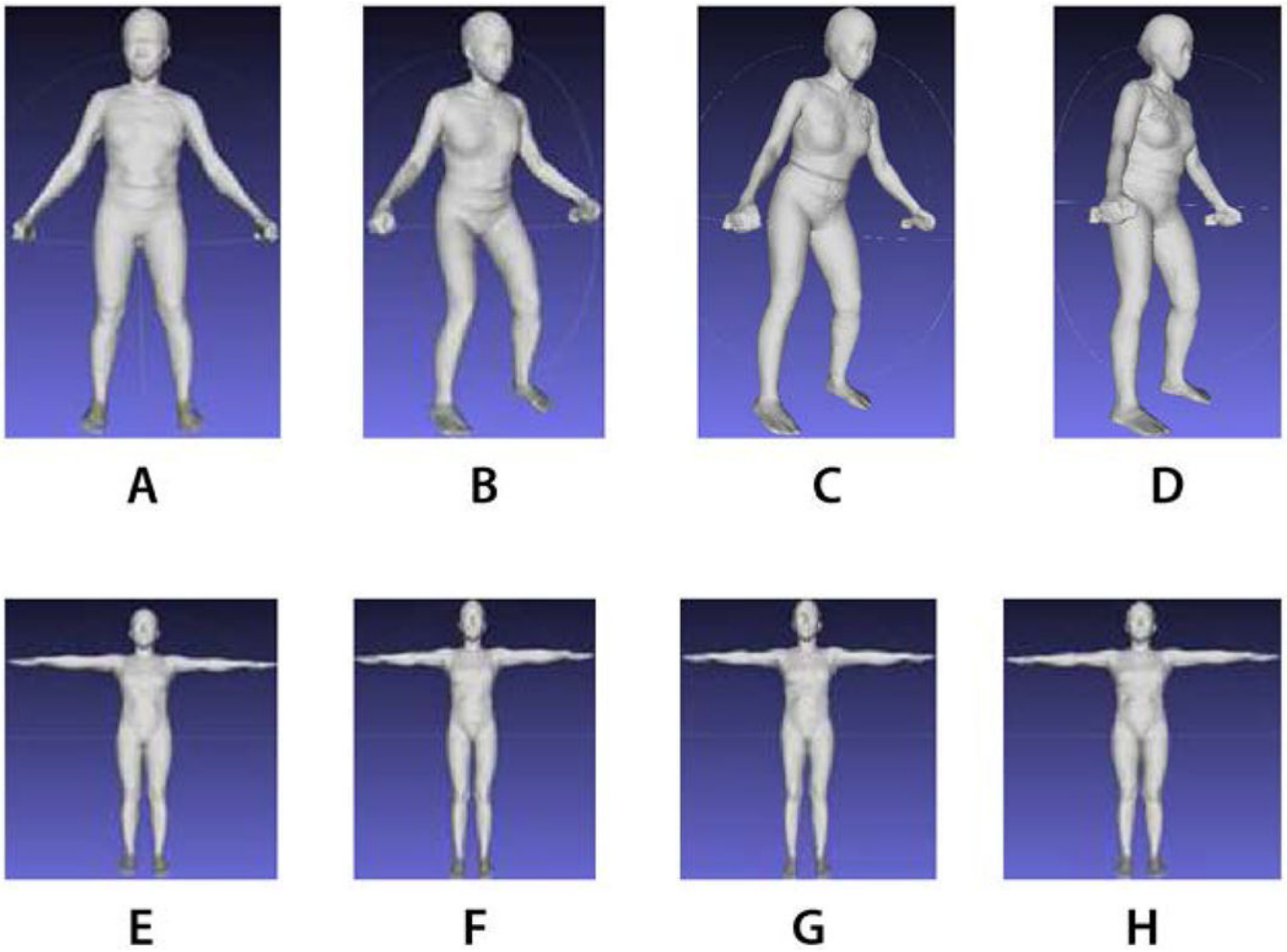


**Figure 1.**

A) Standard A-pose stance on Fit3D. B-D) Alternate A-pose stances on Fit3D. E-H) Reposed meshes A-D. Images A, B, C, and D was a person in different poses. Images, E, F, G, H showed them reposed.

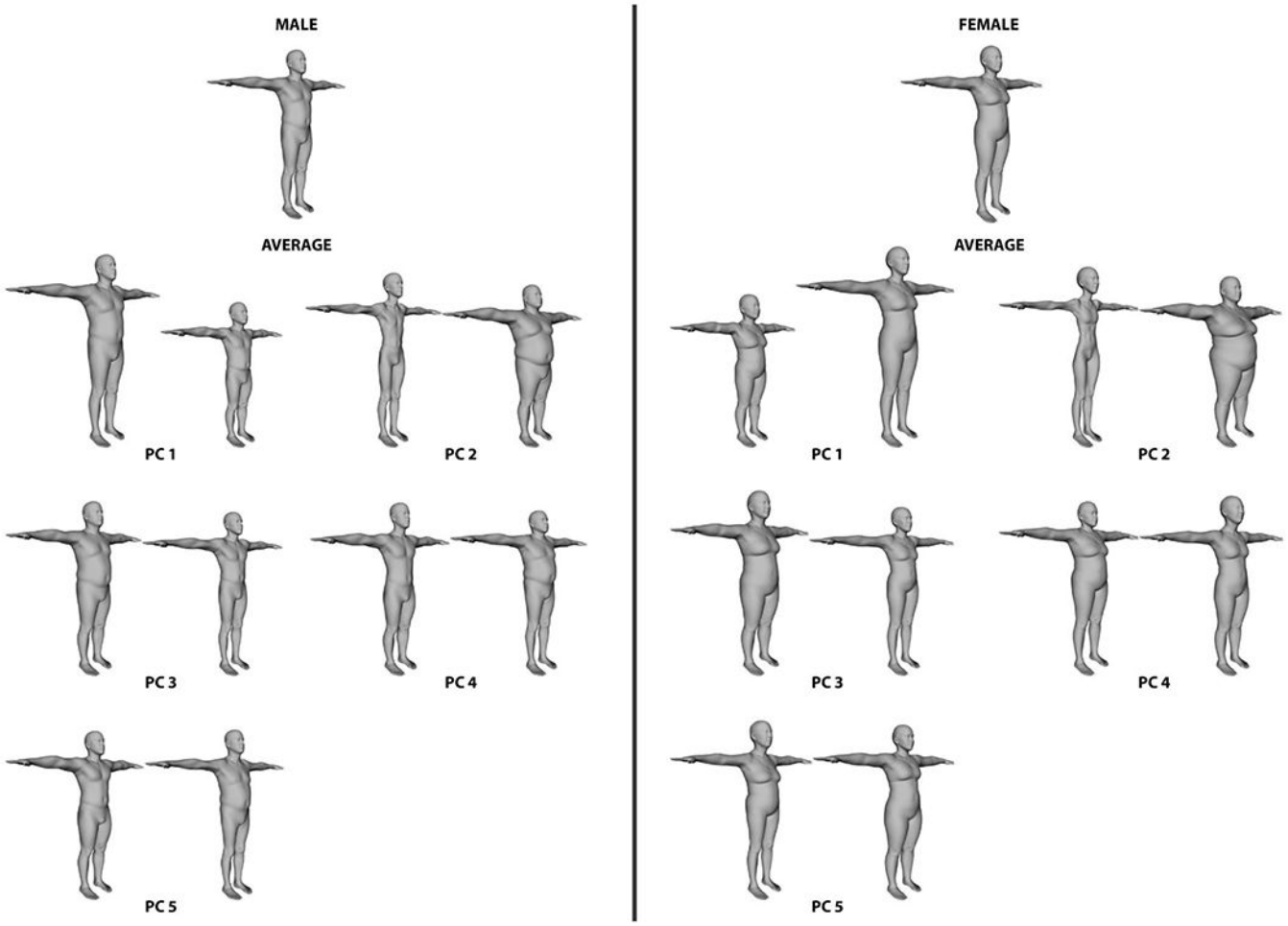


**Figure 2.**

(Top) The mean body shape of males and females in the study sample. These are 110,000-vertex 3D meshes. (Below) The first five principal components of shape variance in males (left) and females (right). Each PC has an according −3 SD (left) and +3 SD (right).

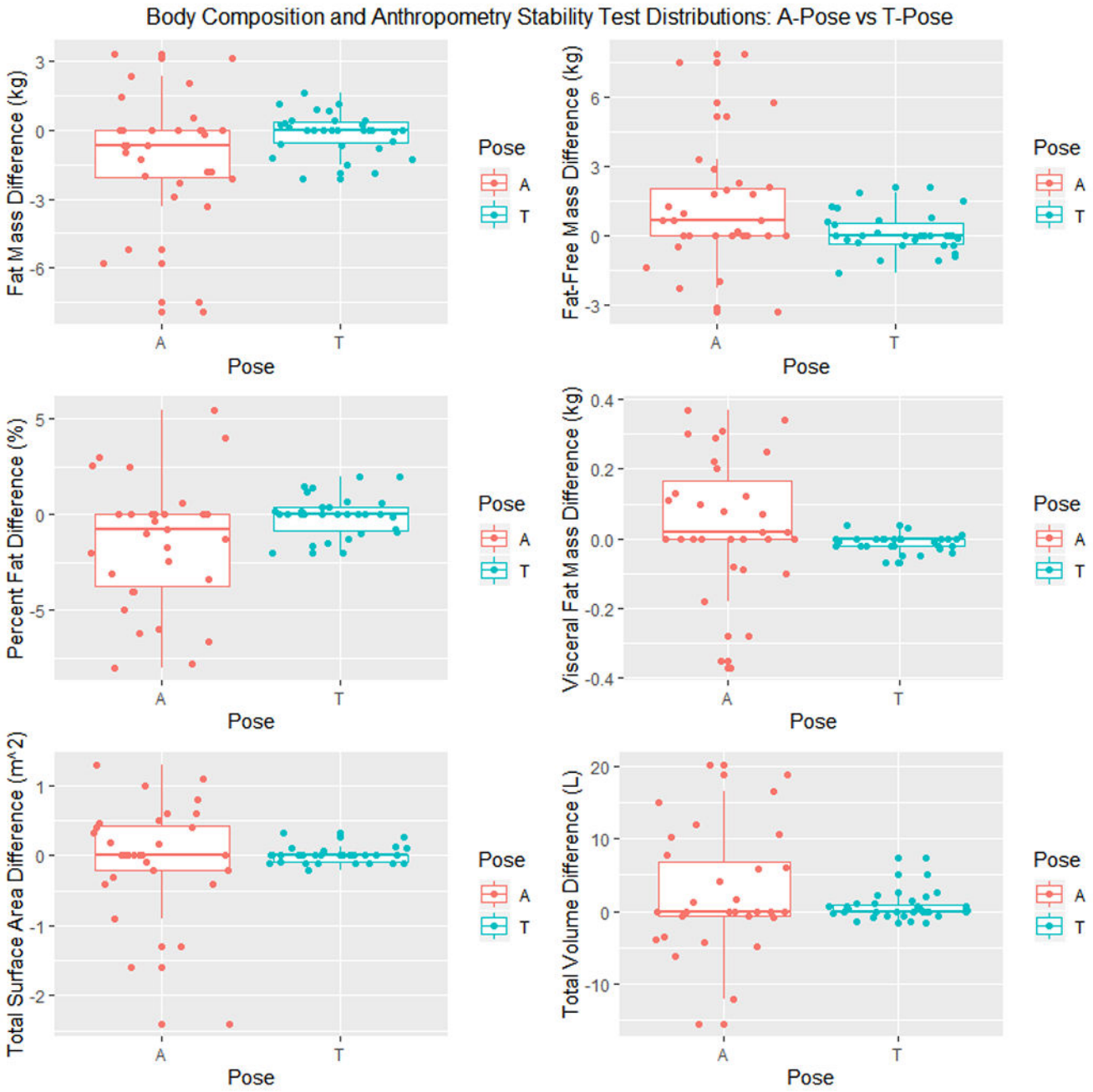


**Figure 3.**

Box and whisker plots. N=8 (male = 4). Each subject had four scans (one with standard protocol and three in various poses). Body composition and anthropometric estimates from the three various poses were subtracted from the standard protocol scan. A-pose and T-pose methods were both used to test the stability of both methods. P-values [FM=0.05, FFM=0.05, %Fat=0.04, VAT=0.09, total surface area=0.99, total volume=0.23].

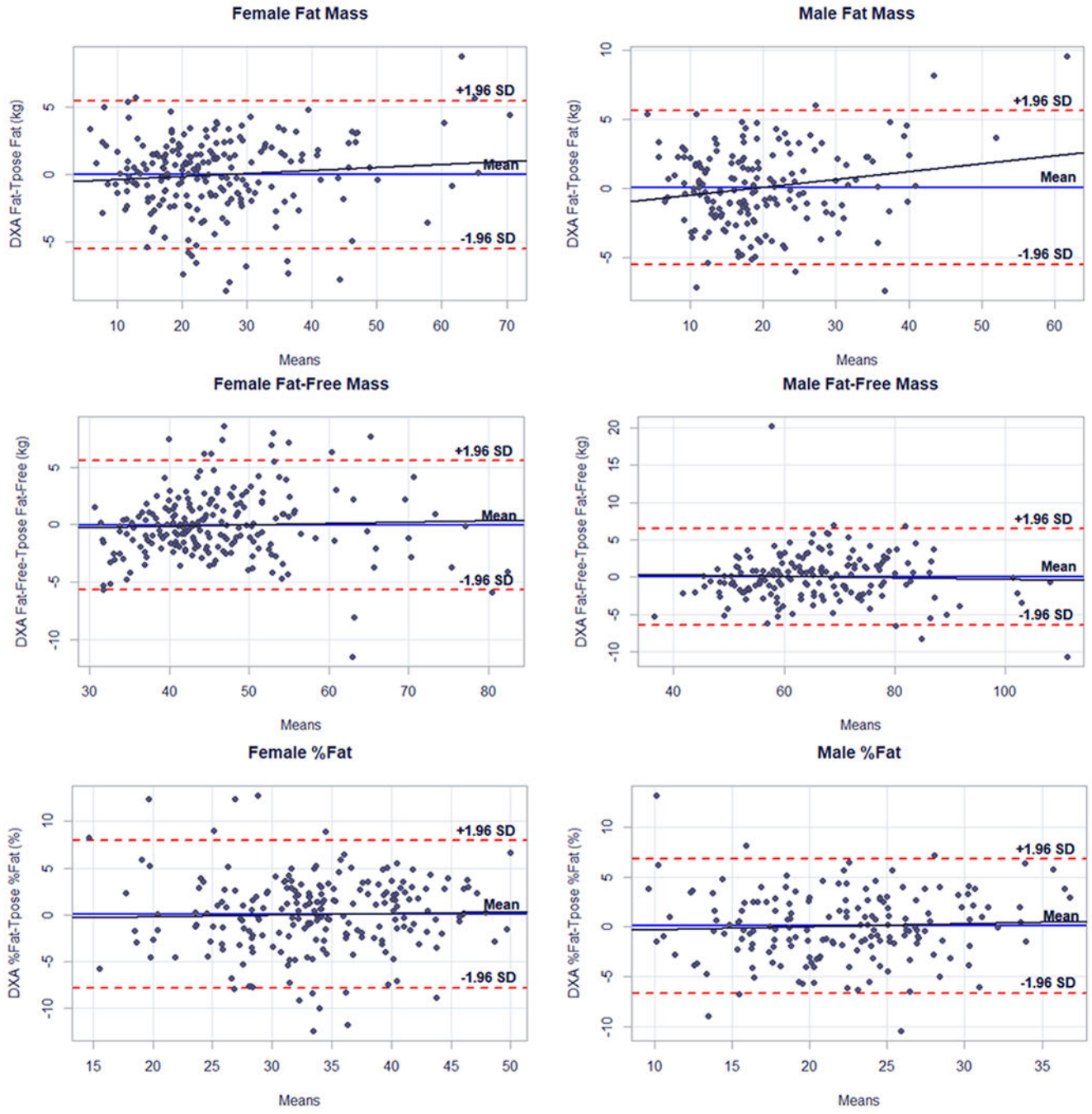


**Figure 4.**
Bland-Altman plots of female and male DXA vs. 3DO T-pose body composition values.

**Table 1.**

Descriptive statistics of training and test samples.

| | | *MALE* | | | | | | | | | *FEMALE* | | | | | | | | |
|---|---|---|---|---|---|---|---|---|---|---|---|---|---|---|---|---|---|---|---|
| **Parameter** | **Units** | **N** | **Mean(SD)** | **Min** | **Max** | **N** | **Mean(SD)** | **Min** | **Max** | **P-Value** | **N** | **Mean(SD)** | **Min** | **Max** | **N** | **Mean(SD)** | **Min** | **Max** | **P-Value** |
| | | **Training** | | | | **Test** | | | | | **Training** | | | | **Test** | | | | |
| Age | years | 167 | 44.1(16) | 18 | 77 | 43 | 43.1(17) | 18.0 | 79.0 | 0.72 | 210 | 46.1(16) | 18 | 74 | 54 | 49.4(16) | 21.0 | 75.0 | 0.18 |
| Height | cm | 167 | 175(8) | 147 | 202 | 43 | 177(6.3) | 165 | 188 | 0.10 | 210 | 162(7.2) | 144 | 181 | 54 | 162(6.5) | 147 | 176 | 0.99 |
| Weight | kg | 167 | 86(21) | 40.6 | 174 | 43 | 86.4(19) | 56.8 | 149 | 0.89 | 210 | 71.5(20) | 38.6 | 153 | 54 | 67.5(17) | 35.4 | 129 | 0.15 |
| BMI | $kg/m^2$ | 167 | 27.9(5.9) | 17 | 52.6 | 43 | 27.4(5.3) | 19.7 | 47.3 | 0.62 | 210 | 27.1(7.4) | 15.9 | 53.1 | 54 | 25.6(6.1) | 14.2 | 46.0 | 0.13 |
| Waist Circ. | cm | 167 | 94.5(16) | 59.4 | 157 | 43 | 94.1(14) | 74.4 | 137 | 0.86 | 210 | 90.2(16) | 65.6 | 157 | 54 | 88.4(14) | 60.5 | 131 | 0.40 |
| Hip Circ. | cm | 167 | 102(11) | 77.1 | 143 | 43 | 102(9.9) | 85.5 | 135 | 0.70 | 210 | 104(14) | 74.5 | 156 | 54 | 101(11) | 74.3 | 128 | 0.13 |
| Arm Circ. | cm | 167 | 34.3(5.2) | 22.5 | 51.3 | 43 | 34.3(4.5) | 26.8 | 44.4 | 0.98 | 210 | 31(7.5) | 17.2 | 96.6 | 54 | 30.4(7.1) | 19.2 | 57.6 | 0.58 |
| Thigh Circ. | cm | 167 | 55.7(7.4) | 37.9 | 84.5 | 43 | 55.9(7.2) | 41.7 | 73.8 | 0.89 | 210 | 53.8(9.3) | 31.4 | 113 | 54 | 52(8.1) | 33.6 | 77.3 | 0.16 |
| WHR | | 167 | 0.9(0.1) | 0.60 | 1.3 | 43 | 0.92(0.08) | 0.79 | 1.10 | 0.82 | 210 | 0.9(0.1) | 0.7 | 1.4 | 54 | 0.87(0.07) | 0.72 | 1.04 | 0.72 |
| WHtR | | 167 | 0.5(0.1) | 0.40 | 0.9 | 43 | 0.53(0.08) | 0.42 | 0.77 | 0.51 | 210 | 0.6(0.1) | 0.4 | 0.9 | 54 | 0.55(0.09) | 0.38 | 0.78 | 0.41 |
| Total Fat Mass | kg | 159 | 19.6(9.3) | 6.1 | 66.4 | 43 | 19.9(9.4) | 7.4 | 48.7 | 0.88 | 210 | 25.4(12) | 6.4 | 72.7 | 53 | 23.3(9.7) | 6.8 | 55.3 | 0.19 |
| Total Lean Mass | kg | 159 | 65.8(13) | 33.7 | 108 | 43 | 66.9(12) | 43.7 | 100 | 0.61 | 210 | 46.2(9.6) | 28.9 | 80.4 | 53 | 44.5(8.8) | 28.6 | 73.0 | 0.21 |
| Percent Fat | % | 159 | 22.2(6.1) | 9.0 | 38.6 | 43 | 22.1(6.4) | 10.2 | 38.7 | 0.97 | 210 | 34.1(7.3) | 12.9 | 53.6 | 53 | 33.3(7.1) | 17.7 | 48.6 | 0.48 |
| FMI | $kg/m^2$ | 159 | 6.4(2.9) | 2.0 | 20.1 | 43 | 6.29(2.9) | 2.4 | 15.5 | 0.84 | 210 | 9.7(4.4) | 2.0 | 24.7 | 53 | 8.9(3.6) | 2.7 | 19.3 | 0.19 |
| FFMI | $kg/m^2$ | 159 | 21.5(3.6) | 14.1 | 35.8 | 43 | 21.3(3.3) | 15.2 | 31.8 | 0.76 | 210 | 17.5(3.2) | 12.2 | 29.1 | 53 | 16.9(2.9) | 11.4 | 27.0 | 0.17 |
| Visceral Fat | kg | 159 | 0.5(0.3) | 0.2 | 1.6 | 43 | 0.45(0.3) | 0.16 | 1.35 | 0.61 | 210 | 0.4(0.3) | 0.1 | 1.3 | 53 | 0.43(0.3) | 0.06 | 1.45 | 0.99 |
| Trunk Fat | kg | 159 | 9.7(5.5) | 2.2 | 33.9 | 43 | 9.61(5.3) | 2.7 | 25.3 | 0.91 | 210 | 11.6(6.3) | 2.5 | 35.6 | 53 | 10.7(5.3) | 2.5 | 26.7 | 0.29 |
| Trunk Lean | kg | 159 | 31.5(6.3) | 15.9 | 51.4 | 43 | 31.6(5.6) | 20.7 | 49.7 | 0.91 | 210 | 22.9(45) | 13.9 | 42 | 53 | 22.1(4.5) | 13.9 | 34.8 | 0.26 |
| Arm Fat | kg | 159 | 1.2(0.6) | 0.4 | 4.5 | 43 | 1.18(0.6) | 0.4 | 3.2 | 0.97 | 210 | 1.6(0.9) | 0.3 | 6.1 | 53 | 1.5(0.7) | 0.4 | 4.0 | 0.16 |
| Arm Lean | kg | 159 | 4.4(1.0) | 2 | 8.3 | 43 | 4.46(1.0) | 2.8 | 6.7 | 0.58 | 210 | 2.4(0.6) | 1.5 | 4.7 | 53 | 2.3(0.5) | 1.5 | 4.1 | 0.29 |
| Leg Fat | kg | 159 | 3.2(1.5) | 1.1 | 11.1 | 43 | 3.38(1.7) | 1.1 | 9.1 | 0.54 | 210 | 4.8(2.2) | 1.2 | 13.1 | 53 | 4.3(1.7) | 1.2 | 10.8 | 0.12 |
| Leg Lean | kg | 159 | 10.7(2.3) | 5.3 | 19.1 | 43 | 11.1(2.2) | 7.01 | 16.2 | 0.39 | 210 | 7.5(1.8) | 4.3 | 14.2 | 53 | 7.1(1.6) | 4.6 | 12.8 | 0.14 |

Abbreviations: Circ. (circumference); WHR (waist to hip ratio); WHtR (waist to height ratio); FMI (fat mass index); FFMI (fat-free mass index)

Circumferences were measured with tape.

Body composition estimates are from DXA.

**Table 2.**

Body composition predictions using whole-body 3DO surface scans. Linear models were trained using 5-fold cross-validation.

| | | | | Model Type | | | | | | | |
|---|---|---|---|---|---|---|---|---|---|---|---|
| | | | | A-Pose PC-Only | | T-Pose PC-Only | | A-Pose PC + Anthro | | T-pose PC + Anthro | |
| **Output Variable** | **Sex** | **N** | **T-Pose PC-Only Model** | **$R^2$** | **RMSE** | **$R^2$** | **RMSE** | **$R^2$** | **RMSE** | **$R^2$** | **RMSE** |
| **Fat Mass** [kg] | M | 159 | PC1, 2, 3, 4, 5, 7, 8, 10, 13 | 0.88 | 3.33 | 0.90 | 2.99 | 0.93 | 2.50 | 0.94 | 2.44 |
| | F | 202 | PC1, 2, 3, 4, 5, 7, 9, 10, 12, 13, 15 | 0.93 | 3.17 | 0.95 | 2.88 | 0.94 | 2.93 | 0.96 | 2.54 |
| **FFM** [kg] | M | 159 | (scale weight) - (predicted FM) | 0.94 | 3.23 | 0.95 | 2.90 | 0.97 | 2.40 | 0.97 | 2.34 |
| | F | 202 | | 0.89 | 3.10 | 0.92 | 2.79 | 0.91 | 2.84 | 0.94 | 2.44 |
| **Percent Fat** [%] | M | 159 | ((predicted FM) / (scale weight)) * 100 | 0.64 | 3.70 | 0.70 | 3.36 | 0.80 | 2.78 | 0.80 | 2.73 |
| | F | 202 | | 0.66 | 4.32 | 0.71 | 3.96 | 0.70 | 4.06 | 0.78 | 3.46 |
| **FMI** [kg/m$^2$] | M | 159 | (predicted FM) / (height)$^2$ | 0.87 | 1.05 | 0.90 | 0.95 | 0.93 | 0.78 | 0.93 | 0.77 |
| | F | 202 | | 0.93 | 1.18 | 0.94 | 1.07 | 0.94 | 1.07 | 0.96 | 0.93 |
| **FFMI** [kg/m$^2$] | M | 159 | (predicted FFM) / (height)$^2$ | 0.92 | 1.05 | 0.93 | 0.95 | 0.95 | 0.78 | 0.95 | 0.77 |
| | F | 202 | | 0.86 | 1.19 | 0.89 | 1.08 | 0.89 | 1.09 | 0.92 | 0.94 |
| **Visceral Fat Mass** [kg] | M | 159 | PC1, 2, 3, 4, 5, 7, 10, 14 | 0.64 | 0.17 | 0.78 | 0.13 | 0.75 | 0.15 | 0.80 | 0.13 |
| | F | 202 | PC2, 3, 4, 5, 6, 8, 11, 12, 13, 14 | 0.73 | 0.14 | 0.78 | 0.13 | 0.79 | 0.13 | 0.80 | 0.13 |
| **Trunk Fat Mass** [kg] | M | 159 | PC1, 2, 3, 4, 5, 8, 10, 14 | 0.90 | 1.78 | 0.92 | 1.62 | 0.94 | 1.44 | 0.95 | 1.31 |
| | F | 202 | PC1, 2, 3, 4, 6, 8, 10, 12, 13, 14 | 0.94 | 1.53 | 0.95 | 1.38 | 0.95 | 1.42 | 0.96 | 1.30 |
| **Trunk FFM** [kg] | M | 159 | PC1, 2, 3, 4, 5, 7, 12 | 0.92 | 1.79 | 0.94 | 1.63 | 0.94 | 1.57 | 0.95 | 1.42 |
| | F | 202 | PC1, 2, 3, 4, 5, 6, 7, 12, 14 | 0.87 | 1.77 | 0.89 | 1.66 | 0.90 | 1.56 | 0.92 | 1.43 |
| **Arms Fat Mass** [kg] | M | 159 | PC1, 2, 3, 4, 5, 7 | 0.84 | 0.26 | 0.84 | 0.25 | 0.90 | 0.21 | 0.91 | 0.20 |
| | F | 202 | PC1, 2, 3, 8, 9, 13, 15 | 0.87 | 0.32 | 0.88 | 0.33 | 0.88 | 0.31 | 0.89 | 0.31 |
| **Arms FFM** [kg] | M | 159 | PC1, 2, 4, 5, 7, 8, 10, 14 | 0.80 | 0.49 | 0.88 | 0.37 | 0.90 | 0.35 | 0.90 | 0.34 |
| | F | 202 | PC1, 2, 4, 5, 11, 13 | 0.66 | 0.35 | 0.75 | 0.31 | 0.75 | 0.30 | 0.78 | 0.29 |
| **Legs Fat Mass** [kg] | M | 159 | PC1, 2, 3, 4, 7, 8, 13 | 0.69 | 0.81 | 0.81 | 0.65 | 0.85 | 0.58 | 0.87 | 0.55 |
| | F | 202 | PC1, 2, 3, 4, 5, 6, 7, 8, 9, 10, 12, 13, 15 | 0.85 | 0.85 | 0.90 | 0.72 | 0.86 | 0.84 | 0.92 | 0.65 |
| **Legs FFM** [kg] | M | 159 | PC1, 2, 3, 4, 5, 6, 11, 12, 14, 15 | 0.88 | 0.81 | 0.90 | 0.73 | 0.94 | 0.60 | 0.92 | 0.67 |
| | F | 202 | PC1, 2, 3, 4, 5, 6, 11, 13, 14, 15 | 0.84 | 0.73 | 0.87 | 0.66 | 0.90 | 0.91 | 0.92 | 0.53 |

| | | | | Model Type | | | | | | | |
|---|---|---|---|---|---|---|---|---|---|---|---|
| | | | | A-Pose PC-Only | | T-Pose PC-Only | | A-Pose PC + Anthro | | T-pose PC + Anthro | |
| **Output Variable** | **Sex** | **N** | **T-Pose PC-Only Model** | **$R^2$** | **RMSE** | **$R^2$** | **RMSE** | **$R^2$** | **RMSE** | **$R^2$** | **RMSE** |
| **Total Surface Area [$m^2$]** | M | 166 | PC1-7, 9, 11, 12 | 0.99 | 0.02 | 0.98 | 0.03 | 0.99 | 0.01 | 0.99 | 0.01 |
| | F | 210 | PC1-3, 5, 6, 8, 12, 14, 15 | 0.96 | 0.04 | 0.98 | 0.03 | 0.99 | 0.01 | 0.99 | 0.01 |
| **Arm Vol [L]** | M | 166 | PC1, 2, 3, 5, 7, 8, 10, 12, 14 | 0.91 | 0.43 | 0.93 | 0.38 | 0.95 | 0.32 | 0.96 | 0.30 |
| | F | 210 | PC1, 2, 3, 5, 7, 8, 11, 12, 14, 15 | 0.92 | 0.41 | 0.93 | 0.35 | 0.96 | 0.29 | 0.97 | 0.27 |
| **Leg Vol** [L] | M | 166 | PC1, 2, 3, 5, 6, 7, 8, 10-15 | 0.91 | 0.92 | 0.96 | 0.62 | 0.97 | 0.54 | 0.98 | 0.49 |
| | F | 210 | PC1-10, 12-15 | 0.95 | 0.85 | 0.96 | 0.73 | 0.96 | 0.70 | 0.97 | 0.58 |
| **Trunk Vol** [L] | M | 166 | PC1-5, 7, 8, 10, 12, 14, 15 | 0.98 | 1.61 | 0.98 | 1.54 | 0.99 | 1.16 | 0.99 | 1.10 |
| | F | 210 | PC1-8, 10-13, 15 | 0.98 | 1.56 | 0.98 | 1.36 | 0.99 | 1.23 | 0.99 | 1.04 |
| **Total Vol** [L] | M | 166 | PC1-5, 7, 8, 10-14 | 0.99 | 2.49 | 0.98 | 2.59 | 0.99 | 0.62 | 0.99 | 1.21 |
| | F | 210 | PC1-6, 8-15 | 0.99 | 2.51 | 0.99 | 2.45 | 0.99 | 1.21 | 0.99 | 1.18 |

Abbreviations: Anthro. (anthropometric); CV (cross-validation); FMI (fat mass index); FFM (fat-free mass); FFMI (fat-free mass index); PCA (principal component analysis); PC (principal component); RMSE, (root mean square error).

Columns noted with (Ng, 2019) used methods described in Ng et al. 2019

**Table 3.**

Test-retest precision of body composition estimates from 3DO and DXA scans

| | | *MALE (n=136)* | | | *FEMALE (n=166)* | | |
|---|---|---|---|---|---|---|---|
| | | ***DXA*** | ***A-Pose*** | ***T-Pose*** | ***DXA*** | ***A-Pose*** | ***T-Pose*** |
| **Outcome** | **Units** | **CV(RMSE)** | | | | | |
| Total Fat Mass | kg | 1.33 (0.25) | 4.86 (0.93) | 2.37 (0.44) | 0.95 (0.23) | 3.31 (0.79) | 2.24 (0.55) |
| Total Fat-Free Mass | kg | 0.51 (0.34) | 1.41 (0.93) | 0.68 (0.44) | 0.61 (0.27) | 1.74 (0.79) | 1.21 (0.55) |
| Total Percent Fat | % | 1.31 (0.28) | 5.39 (1.17) | 2.62 (0.57) | 0.98 (0.33) | 3.57 (1.19) | 2.41 (0.82) |
| Fat Mass Index | $kg/m^2$ | 1.35 (0.08) | 4.94 (0.31) | 2.38 (0.15) | 0.95 (0.09) | 3.34 (0.30) | 2.27 (0.21) |
| Fat-Free Mass Index | $kg/m^2$ | 0.50 (0.11) | 1.43 (0.31) | 0.68 (0.15) | 0.62 (0.10) | 1.76 (0.30) | 1.23 (0.21) |
| Visceral Fat Mass | kg | 7.36 (0.03) | 10.9 (0.05) | 4.99 (0.02) | 7.91 (0.03) | 6.24 (0.03) | 4.64 (0.02) |
| Trunk Fat | kg | 2.56 (0.24) | 5.58 (0.52) | 2.38 (0.22) | 2.02 (0.23) | 3.26 (0.35) | 1.82 (0.21) |
| Trunk Lean | kg | 1.12 (0.35) | 1.68 (0.53) | 1.05 (0.33) | 1.11 (0.25) | 1.55 (0.35) | 1.15 (0.26) |
| Arm Fat | kg | 3.08 (0.04) | 4.84 (0.06) | 3.00 (0.03) | 2.90 (0.05) | 2.88 (0.04) | 4.29 (0.07) |
| Arm Lean | kg | 1.52 (0.07) | 3.22 (0.14) | 2.01 (0.09) | 2.06 (0.05) | 2.43 (0.06) | 2.95 (0.07) |
| Leg Fat | kg | 2.32 (0.07) | 4.46 (0.14) | 4.63 (0.14) | 1.44 (0.07) | 5.72 (0.18) | 3.45 (0.16) |
| Leg Lean | kg | 1.22 (0.13) | 2.48 (0.27) | 1.56 (0.17) | 1.13 (0.08) | 2.44 (0.18) | 1.67 (0.12) |
| Total Surface Area | $m^2$ | -- | 0.69 (0.01) | 0.58 (0.01) | -- | 0.77 (0.01) | 0.63 (0.01) |
| Arm Volume | L | 1.62 (0.09) | 2.38 (0.13) | 1.50 (0.08) | 1.81 (0.07) | 2.23 (0.09) | 1.83 (0.07) |
| Leg Volume | L | 1.02 (0.14) | 2.34 (0.33) | 1.35 (0.19) | 0.94 (0.12) | 3.16 (0.39) | 1.88 (0.23) |
| Trunk Volume | L | 0.91 (0.37) | 1.39 (0.58) | 1.01 (0.41) | 0.94 (0.32) | 1.86 (0.63) | 1.16 (0.40) |
| Total Volume | L | 0.37 (0.31) | 1.21 (1.05) | 0.95 (0.82) | 0.27 (0.19) | 1.59 (1.13) | 1.27 (0.91) |

Duplicate 3DO and DXA scans were each taken with repositioning.

Results are from the PC-only equations

Abbreviations: RMSE (root mean square error); CV (coefficient of variation)

**Table 4.**

Test set results for body composition prediction equations

| | | | *MALE (n=42)* | | *FEMALE (n=53)* | |
|---|---|---|---|---|---|---|
| | | | ***A-Pose*** | ***T-Pose*** | ***A-Pose*** | ***T-Pose*** |
| **Model** | **Outcome** | **Units** | **$R^2$ (RMSE)** | | **$R^2$ (RMSE)** | |
| PC | Total Fat Mass | kg | 0.78 (4.48) | 0.89 (3.10) | 0.93 (2.72) | 0.92 (2.70) |
| | Total Fat-Free Mass | kg | 0.88 (4.38) | 0.94 (3.11) | 0.90 (2.73) | 0.91 (2.70) |
| | Total Percent Fat | % | 0.39 (5.14) | 0.70 (3.58) | 0.64 (4.17) | 0.62 (4.44) |
| | Fat Mass Index | $kg/m^2$ | 0.76 (1.45) | 0.88 (1.01) | 0.92 (1.03) | 0.92 (1.02) |
| | Fat-Free Mass Index | $kg/m^2$ | 0.82 (1.41) | 0.91 (1.02) | 0.88 (1.04) | 0.88 (1.02) |
| | Visceral Fat Mass | kg | 0.64 (0.17) | 0.71 (0.15) | 0.72 (0.16) | 0.76 (0.15) |
| | Trunk Fat | kg | 0.84 (2.13) | 0.93 (1.41) | 0.95 (1.25) | 0.94 (1.34) |
| | Trunk Lean | kg | 0.86 (2.21) | 0.85 (2.23) | 0.87 (1.63) | 0.90 (1.45) |
| | Arm Fat | kg | 0.72 (0.31) | 0.74 (0.29) | 0.88 (0.26) | 0.85 (0.28) |
| | Arm Lean | kg | 0.71 (0.56) | 0.79 (0.48) | 0.70 (0.29) | 0.79 (0.25) |
| | Leg Fat | kg | 0.66 (1.00) | 0.77 (0.80) | 0.82 (0.71) | 0.84 (0.67) |
| | Leg Lean | kg | 0.87 (0.80) | 0.87 (0.79) | 0.78 (0.74) | 0.83 (0.66) |
| | Total Surface Area | $m^2$ | 0.98 (0.03) | 0.98 (0.03) | 0.96 (0.04) | 0.98 (0.03) |
| | Arm Volume | L | 0.92 (0.35) | 0.93 (0.33) | 0.92 (0.34) | 0.94 (0.29) |
| | Leg Volume | L | 0.91 (1.05) | 0.96 (0.66) | 0.92 (0.85) | 0.94 (0.71) |
| | Trunk Volume | L | 0.97 (1.77) | 0.97 (1.58) | 0.98 (1.32) | 0.99 (1.07) |
| | Total Volume | L | 0.98 (2.84) | 0.98 (2.36) | 0.99 (2.07) | 0.98 (2.29) |
| PC + A | Total Fat Mass | kg | 0.88 (3.37) | 0.88 (3.22) | 0.94 (2.37) | 0.93 (2.58) |
| | Total Fat-Free Mass | kg | 0.93 (3.38) | 0.93 (3.21) | 0.93 (2.37) | 0.92 (2.58) |
| | Total Percent Fat | % | 0.64 (3.95) | 0.71 (0.53) | 0.69 (3.82) | 0.68 (4.06) |
| | Fat Mass Index | $kg/m^2$ | 0.87 (1.10) | 0.88 (1.03) | 0.94 (0.89) | 0.93 (0.98) |
| | Fat-Free Mass Index | $kg/m^2$ | 0.89 (1.10) | 0.90 (1.03) | 0.91 (0.90) | 0.89 (0.98) |
| | Visceral Fat Mass | kg | 0.72 (0.15) | 0.74 (0.15) | 0.75 (0.15) | 0.78 (0.14) |
| | Trunk Fat | kg | 0.89 (1.78) | 0.93 (1.42) | 0.94 (1.30) | 0.94 (1.34) |
| | Trunk Lean | kg | 0.90 (1.84) | 0.89 (1.93) | 0.89 (1.51) | 0.90 (1.45) |
| | Arm Fat | kg | 0.77 (0.28) | 0.75 (0.29) | 0.89 (0.25) | 0.88 (0.26) |
| | Arm Lean | kg | 0.85 (0.41) | 0.84 (0.41) | 0.77 (0.26) | 0.83 (0.23) |
| | Leg Fat | kg | 0.82 (0.74) | 0.81 (0.72) | 0.82 (0.71) | 0.84 (0.68) |
| | Leg Lean | kg | 0.92 (0.61) | 0.91 (0.68) | 0.86 (0.59) | 0.88 (0.57) |
| | Total Surface Area | $m^2$ | 0.99 (0.01) | 0.99 (0.01) | 0.99 (0.01) | 0.99 (0.01) |
| | Arm Volume | L | 0.97 (0.22) | 0.97 (0.22) | 0.68 (0.69) | 0.73 (0.63) |
| | Leg Volume | L | 0.97 (0.62) | 0.99 (0.54) | 0.95 (0.69) | 0.97 (0.51) |
| | Trunk Volume | L | 0.99 (1.20) | 0.99 (1.04) | 0.98 (1.26) | 0.99 (0.96) |
| | Total Volume | L | 0.99 (0.71) | 0.99 (0.81) | 0.99 (0.84) | 0.99 (1.98) |

Test set participants were withheld from the training set.

Abbreviations: PC (principal component), PC + A (principal component + anthropometry)